LIQUID-PHASE DIFFUSION BONDING: TEMPERATURE EFFECTS AND SOLUTE REDISTRIBUTION IN HIGH TEMPERATURE LEAD-FREE COMPOSITE SOLDERS

S.M. Choquette[1,2] and I.E. Anderson[1,2]
1: Division of Materials Sciences and Engineering, Ames Laboratory (USDOE), Iowa State University, Ames, IA 50011.
2: Materials Science and Engineering Department, Iowa State University, Ames, IA 50011.

ABSTRACT

Liquid-phase diffusion bonding (LPDB) is being studied as the primary phenomena occurring in the development of a high temperature lead-free composite solder paste composed of gas-atomized Cu-10Ni, wt.% (Cu-11Ni, at.%) powder blended with Sn-0.7Cu-0.05Ni-0.01Ge (Sn-1.3Cu-0.1Ni-0.02Ge, at.%) Nihon-Superior SN100C solder powder. Powder compacts were used as a model system. LPDB promotes enhanced interdiffusion of the low-melting alloy matrix with the solid Cu-10Ni reinforcement powder above the matrix liquidus temperature. The initial study involved the effective intermetallic compound (IMC) compositions and microstructures that occur at varying reflow temperatures and times between 250-300°C and 30-60s, respectively. Certain reflow temperatures encourage adequate interdiffusion to form a continuous highly-conductive network throughout the composite solder joints. The diffusion of nickel, in particular, has a disperse pattern that foreshadows the possibility of a highly-conductive low-melting solder that can be successfully utilized at high temperatures.

INTRODUCTION

The development of high-temperature lead-free solders is becoming increasingly crucial for use in power electronics in the automotive, aerospace, military, and energy production industries [1,2]. The currently used high-temperature solders are Pb-5Sn, wt.% (Pb-8.4Sn, at.%) or Pb-10Sn (Pb-16Sn, at.%) which melt around 300°C and Au-20Sn (Au-29Sn, at.%) which melts at 280°C [3]. A typical solder reflow cycle [Fig.1] will have a peak reflow temperature 20°C to 40°C above the melting point of the solder; therefore, the current typical high temperature solders have reflow temperatures around 330°C or 310°C, respectively [3,4]. The operating temperatures of these solders are usually less than 250°C, but it is critical that the solder be able to survive hierarchical solder reflow throughout all stages of lower temperature reflow processing [1].

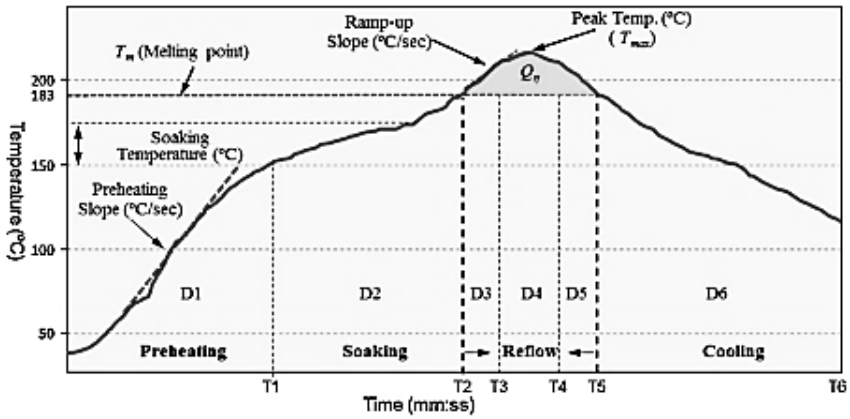

Figure 1: *A typical solder reflow thermal cycle profile [5]*

Our priority was to create a lead-free version of these high-Pb solder alloys that used equal or lower processing temperatures, but could still withstand high operating temperatures. The key to this was to find a suitable system with a lower melting temperature, so that the reflow temperature could also be lower. At this lower reflow temperature, however, the solder needed the ability to evolve to a microstructure with high-temperature stability. An important attribute of any successful substitute for the high-Pb solders is a practical set of mechanical properties that avoids brittle phases, which is a problem for several of the current alternatives, including another type of composite paste approach that uses pure copper powder or pure nickel powder as a filler powder [3]. In addition, a practical cost should be associated with a successful solder, unlike the Au-Sn solder system that seems to meet some desirable characteristics, but certainly has a cost issue.

With today's increased power pumping through electronics, higher operating temperatures can contribute to brittleness in solder joints by several mechanisms upon thermal cycling [3,6,7]. In the past, this cracking did not occur because the microstructures formed by lead and tin did not consist of any brittle intermetallic compounds. Now, however, lead use is becoming much more restricted due to RoHS [1,8,9]. In our original concept [Fig. 2] for a new type of Pb-free composite solder paste, borrowed from earlier work on 4th element additions to Sn-Ag-Cu (SAC) solder alloys for improved high temperature stability [10,11], a series of high temperature (330˚C) reflow tests, coupled with extended thermal aging at 250˚C, were conducted with several types of Cu-alloy substrates in contact with a single type of Sn-Cu-Ni solder [Fig.3]. This test design was intended to simulate an aggressive test of "drop-in" application of the composite paste formulations with much more exposure to very high use temperature (250˚C) than expected in typical applications.

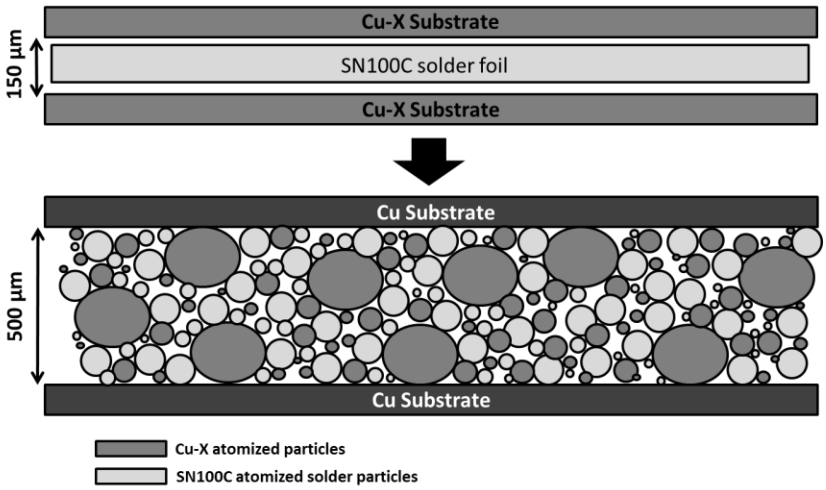

Figure 2: *Top: Schematic of the model test, allowing selection of the element to alloy into the Cu filler. Bottom: Final composite solder paste that joins two Cu substrates. (Results of test model shown in Fig. 3)*

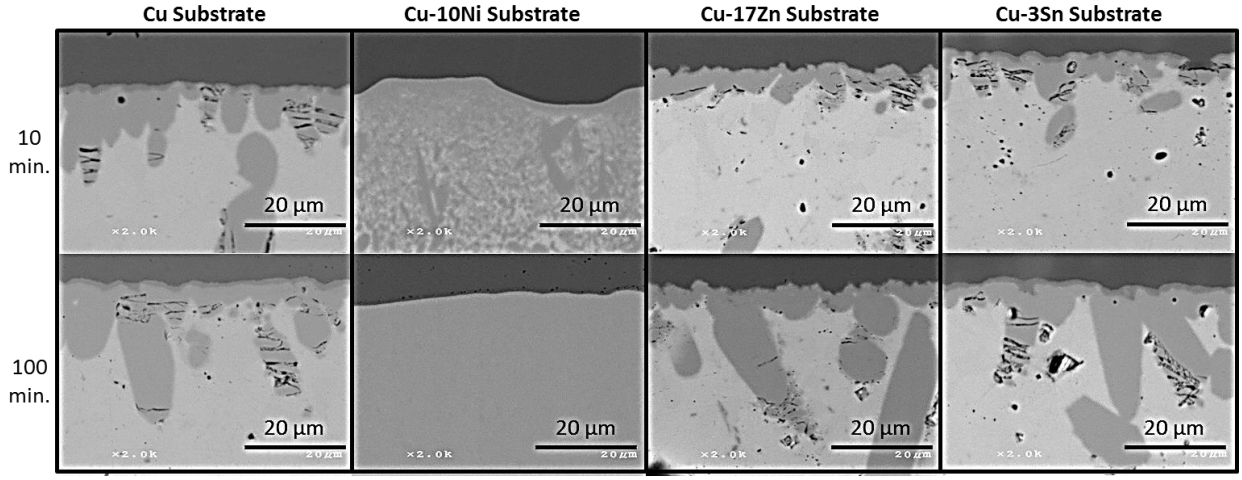

Figure 3: *Microstructures of SN100C on four types of substrate, aged at 10 and 100 minutes, where horizontal lines in the intermediate gray regions indicate cracking. Columns labeled by material type; rows labeled by aging time. (Scale bar = 20µm)*

From microstructural analysis of the resulting joints, nickel was selected as the most promising element to alloy into the Cu filler phase because of its unusual alloying behavior with the Sn-Cu-Ni solder matrix phase in our studies. More specifically, the model joint sample microstructures in Fig. 3 clearly showed that the use of the Cu-10Ni substrate produced the only crack-free IMC during the aging treatments, as well as the ability to rapidly and uniformly spread this IMC across the joint gap. While the effectiveness of Ni to decrease the brittleness of the η-phase (Cu_6Sn_5) IMC formed by copper and tin [6,7] was certainly known, the ability of a local source of excess Ni (from the Cu-10Ni substrate) to promote rapid uniform growth across the joint was not expected and appeared to be very beneficial for our purposes.

In further detail, Fig. 3 shows the microstructures seen during conceptual testing of a composite solder system where the solder joint substrates (shown in the top of each micrograph in Fig. 3) would become the pre-alloyed powder filler phase that is bonded by a low-melting Pb-free solder alloy (Sn-Cu based) matrix phase. The intermediate gray phase/region in each case is the IMC that forms during soldering. Cracking occurs in the intermetallic compounds (IMCs) with pure Cu and the other Cu-alloy types tested except for Cu-Ni. The $(Cu,Ni)_6Sn_5$ IMC growth front in the image second from the left in Fig. 3 is much

more dispersed in its advance, becomes fully transformed compared to the other IMCs upon aging, and has no internal cracking. After 100 minutes of aging of the Cu-10Ni substrate joint, the $(Cu,Ni)_6Sn_5$ phase became a single phase across the entire solder joint, albeit its tendency of joint centerline cracking (not shown in Fig. 3) with these long aging times at 250˚C. Research by Nogita et al. and Kao et al. have shown the composition of this phase can vary between 1 and 12 at.% Ni, while still being effective at reducing the brittleness of the IMC. The most preferred stoichiometry was determined to be $Cu_{5.5}Ni_{0.5}Sn_5$ [6,12,13].

The copper-tin phase diagram shows the important task that nickel must perform in this alloy system. On the Sn-Cu phase diagram, Cu_6Sn_5 is seen existing as two allotropic phases. Cu_6Sn_5 (η) is the high temperature phase and Cu_6Sn_5' (η') is the low temperature phase. The low temperature phase is monoclinic, and the high temperature phase is hexagonal [6,7,12]. The fact that the interfacial Cu_6Sn_5 (η) IMC forms during reflow without excessive porosity shows that there is adequate wetting and bonding of all of the substrate alloys by the solder alloy, but the tendency for cracking of the resulting IMC in the solder joints of Fig. 3 appears to be linked to the allotropic phase transformation on cooling to Cu_6Sn_5' (η') [7,9,14,15].

The Sn-Cu-Ni ternary eutectic system is one of the most popular Pb-free solder systems currently being studied for electronic assembly at increased reflow temperatures (+10˚C) compared to SAC solders [3,6,7,12]. In this particular case, when a Sn-Cu near-eutectic solder cools to 186°C, Nogita et al. describes how the IMC allotropically transforms from the hexagonal phase to the monoclinic phase. By adding nickel, however, the high temperature phase becomes stabilized, stopping this transformation upon cooling to room temperature, where the η-phase (hexagonal) is retained [6,7,16]. If the phase transformation to monoclinic on cooling is allowed to occur, it can cause cracking in newly formed Cu_6Sn_5'-phases near an external surface in the joint. This is due to a volume decrease of about 2.15% that causes stress in the intermetallic layers and is relieved by layered cracking, as observed in Fig. 3 [6,7]. In addition to removing an abrupt volume change from the allotropic transformation, extra slip systems (and ductility) result from retaining the hexagonal allotrope, making this hexagonal phase much more attractive for engineering use.

Thus, as a key innovative aspect of this work, the concept of blending together two types of Ni-containing powders (gas-atomized Cu-10Ni wt.% powder particles and gas atomized solder powder of Nihon Superior's SN100C) to form a composite paste was developed. From the model results for the Cu-10Ni substrate (see Fig. 3) that showed the tendency for a rapidly-growing, dispersed IMC that completely consumed the solder matrix, we hypothesized that a low-melting composite solder paste could be developed from this system. These model system results also suggested that joints formed from such a paste could be successfully utilized at high temperatures once the matrix (SN100C) solder alloy was sufficiently transformed into the Cu_6Sn_5 (η-phase) by providing localized sources of excess Ni from heavily loaded Cu-10Ni powder in the composite microstructure.

To test this concept before going through the compounding of a full paste sample, the intended dual-powder composite model was produced as a porous compact that was infiltrated by a typical flux for the SN100C solder and reflowed. These model joints were useful for microstructure evaluation to study the effects of varying reflow time and temperature. The aim was to demonstrate that the composite solder joint microstructure could benefit from well-dispersed nickel additions that originated in the solder powders and, in excess, in the Cu-10Ni powder. Thus, it was intended to rapidly form a ductile intermetallic compound that could serve as a strong, crack-free matrix phase for the resulting highly-conductive Cu-10Ni particle network [1,4,17,18,19].

EXPERIMENTAL PROCEDURE

Composite Model Preparation

Model composite solder joints were produced with a variety of blends of gas-atomized Cu-10Ni wt.% powder and Sn-0.7Cu-0.05Ni+0.01Ge wt.% Nihon-Superior SN100C solder powder, according to the combinations listed in Fig. 4. The Cu-10Ni powders were of the size range 25 - 32 µm (similar to Type 4 solder powder) and the SN100C powders were of the size range 5-15 µm (Type 6). The powder size (as illustrated in Fig. 4) of our Cu-Ni was chosen to be larger than the SN100C, so as to maximize surface area for wetting and minimize IMC formation [20]. The powders were dehydrated to reduce clumping for 1 hour at 100°C and blended with a multiple axis blender for approximately 20 minutes. The blended powders were then compressed, using a cold isostatic press (CIP) at a pressure of 20 ksi, into 5 mm diameter rods with densities of 73.1%. The resulting compacted powder rods were cut into approximately two millimeter discs, and leveled with 320 grit paper for use as solder compacts. The chosen density allowed the CIPed powder compacts to soak up flux in order to imitate a solder paste.

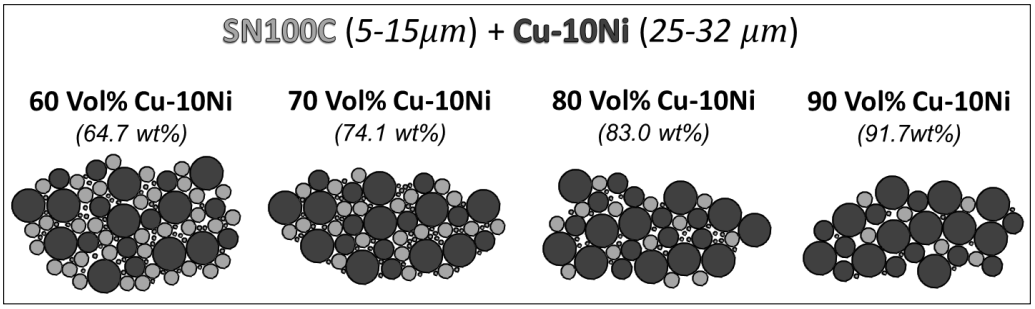

Figure 4: *Volume percent and relative size comparison of blended powders tested for paste use, where the light material is the SN100C and the dark material is the Cu-10Ni.*

Composite Model Reflow

The flux-soaked powder compacts were then tested using the setup in Fig. 5. The compacts were placed between two boron-nitride coated stainless steel plates to optimize the heating of the solder compacts. The stainless steel plates provided a heat sink to quickly heat the solder compact, while the boron nitride coating (a highly thermally-conductive ceramic) prevented any interaction of the solder with the stainless steel. The plates were kept in the furnace overnight to reach the desired temperatures prior to testing. The setup [Fig. 5.1] was located in a furnace and tested with peak reflow temperatures of 250°C, 275°C, and 300°C, along with peak reflow times of 30 and 60 seconds.

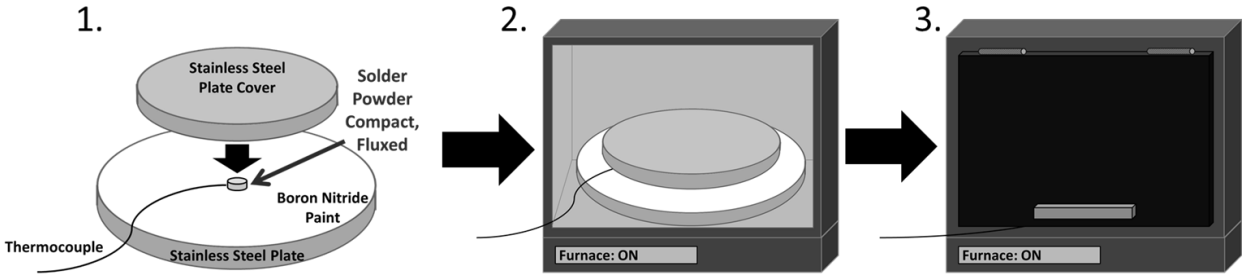

Figure 5: *1. Schematic setup of composite solder compact; 2. Schematic view of the setup within the box furnace; 3. Schematic view of the box furnace closed for experimentation*

Fig. 6 contains the recorded reflow cycles of the experiment, which match well with reflow cycles from literature [5,7]. The solder paste models were cooled at about 1.5°C per second, determined by earlier work [10], by placing them on a copper block at room temperature to cool.

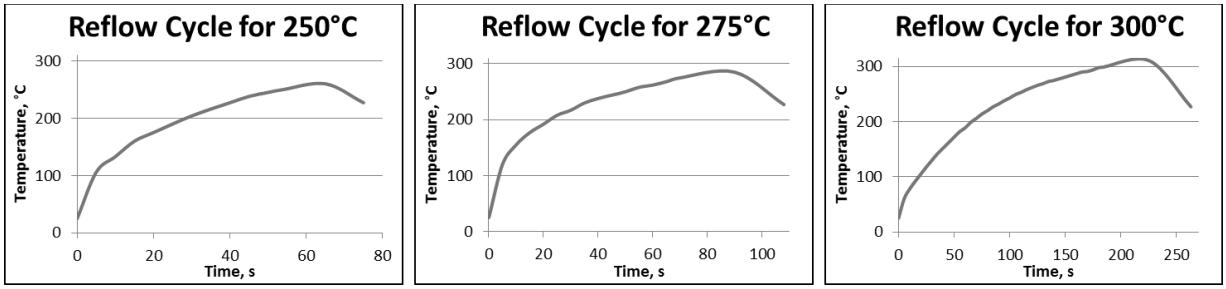

Figure 6: *Time versus temperature plots representing average measured thermal cycles at each reflow temperature*

At random, of the 6 reflow combinations, four were repeated three times and two were repeated twice. At least 16 micrographs of the same magnification were taken and analyzed for each tested sample. After analysis, the best ratio of powders was determined to be 70 volume percent Cu-10Ni with 30 volume percent SN100C. This combination resulted in the best continuous Cu-Ni conductive network while not sacrificing the tin alloy matrix needed to wet the particles together to form our important IMC. Therefore, going forward, the following results are reported for the model containing 70 volume percent Cu-10Ni.

RESULTS

Fig. 7 contains the resulting micrographs (in Z contrast) for each combination of reflow time and temperature tested. From these images, the microstructures look very similar to each other. Therefore, the same micrographs (in Z contrast) are given in Fig. 8 at a higher magnification. The darkest colored regions are the Cu-Ni, the intermediate gray phase is the IMC, and the lightest phase is the residual SN100C matrix. Again, it is hard to differentiate the microstructures just by the naked eye, although the clearest overall impression is that the shortest time and lowest temperature reflow cycle gives an obviously higher volume fraction of Cu-10Ni spherical particles compared to the 300°C and 60s reflow cycle sample microstructure. In addition, what we *are* able to observe from Fig. 7 and Fig. 8 is the lack of cracking in the IMC and the lack of any apparent Kirkendall voids [19,21].

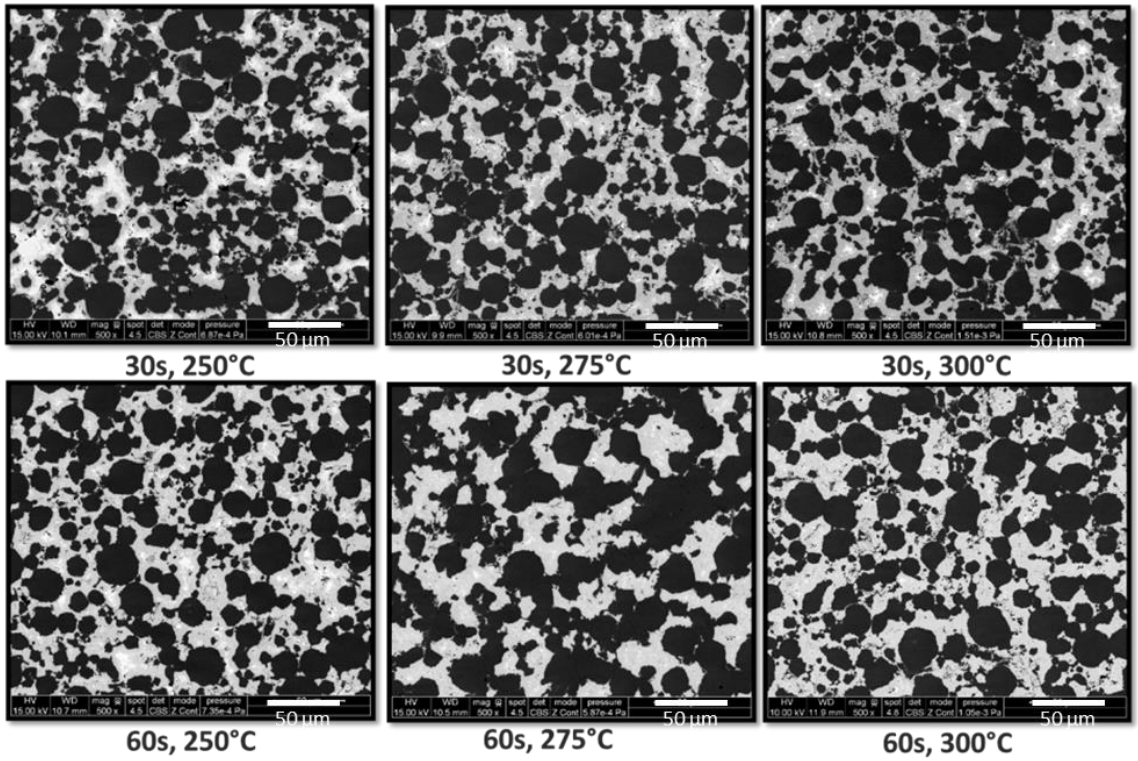

Figure 7: *SEM (backscatter) micrographs for each combination of reflow times and temperatures with a scale bar of 50 µm.*

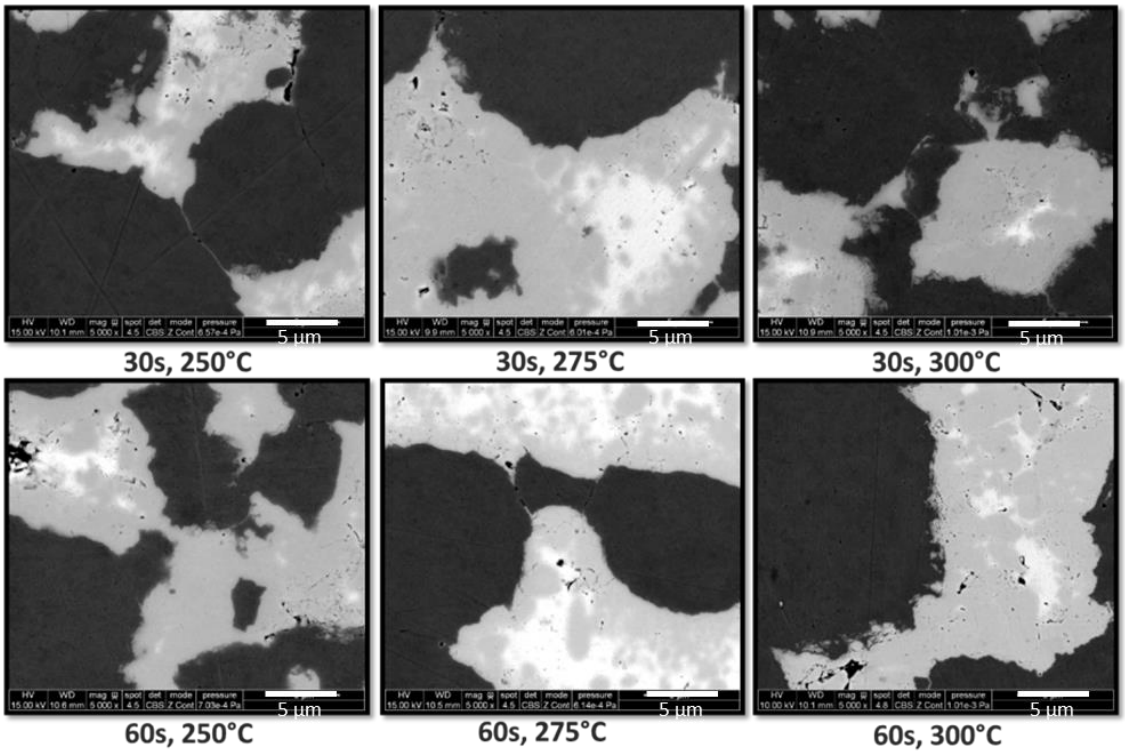

Figure 8: *SEM (backscatter) micrographs for each combination of reflow times and temperatures with a scale bar of 5 µm*

The image analysis and quantitative metallography of 16 micrographs per sample gave us the averages shown in Fig. 9 for the area percent of the phases present in the average microstructure. With shorter reflow cycles, there was a slightly larger content of residual tin alloy left in the microstructures (~ 4 at.%). This phase would melt upon reheating to above 227°C, but should then continue its interdiffusion with the Cu-Ni particles during each successive reflow cycle. As shown in the pie charts of Fig. 9, the amount of residual tin can be decreased with longer reflow cycles, if desired. However, longer cycling decreases the amount of reinforcement powder, which is by far the best conductive path through the joint. Therefore, in order to maximize the content of our highest conducting phase Cu-10Ni, the shorter reflow times are recommended for this composite solder paste.

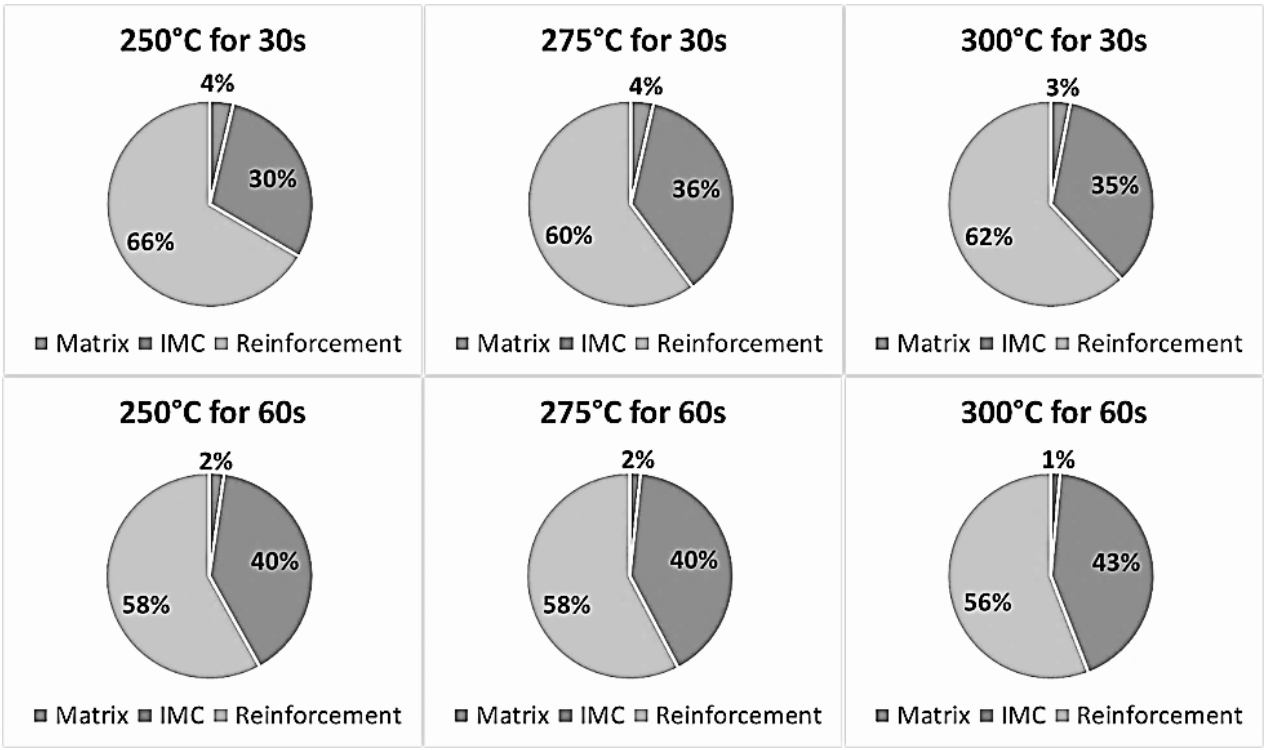

Figure 9: *The average percent area of each phase measured for each reflow combination using quantitative metallography.*

Fig. 10 shows the results of EDS analysis for each reflow combination. These values stayed fairly consistent between reflow tests. The slight copper and nickel in the matrix of each graph (an average of 3.0 at.% Cu and 0.5 at.% Ni) was expected because our matrix originally consisted of SN100C, which contains 0.35 at.% Cu (0.7 wt.%) and 0.02 at.% Ni (0.05 wt.%). The content of Ni in the $(Cu,Ni)_6Sn_5$ IMC varies between 3.4 and 5.6 at.%, which matches well with literature [6,7]. The composition of the reinforcement powders stayed at an average of 10.5 at.% Ni (9.78 wt.%), as expected, because the reflow temperature that this model paste reached was only a quarter of the melting temperature of Cu-10Ni wt.%.

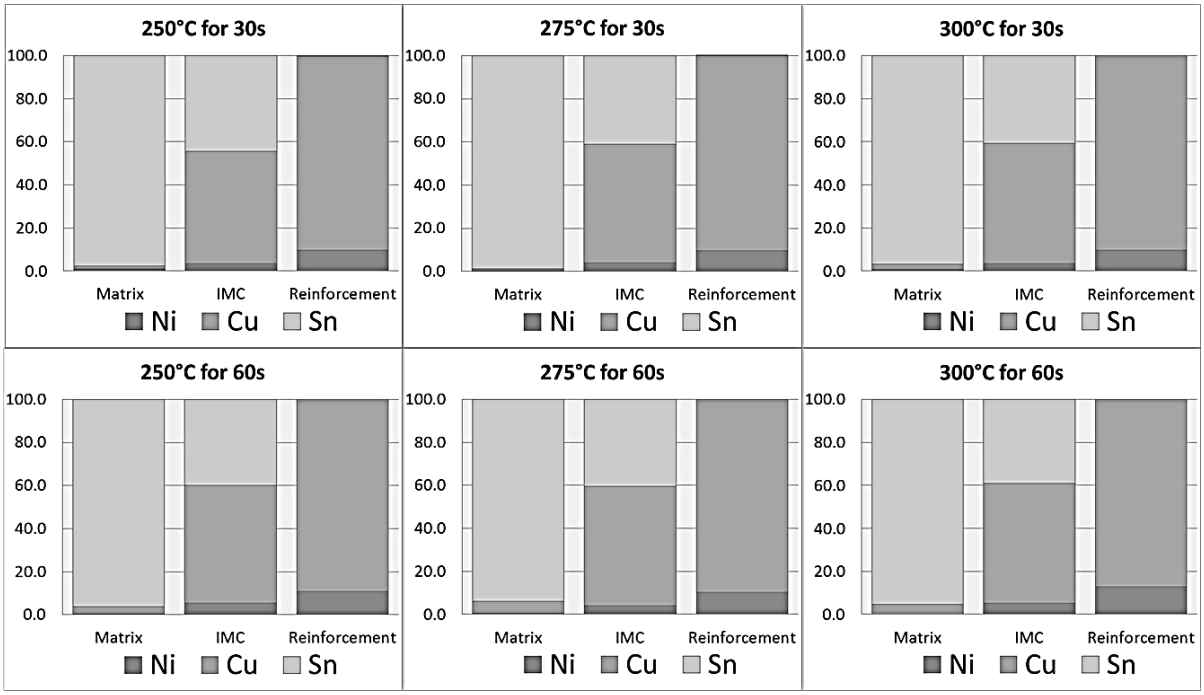

Figure 10: *The average composition (at.%) determined by EDS of each reflow combination.*

DISCUSSION

Within this composite solder of high-melting Cu-Ni "filler" and low melting SN100C "matrix" solder alloy, a process some have called "transient liquid phase sintering" (TLPS) was expected, where the Sn component of the SN100C matrix alloy would diffuse preferentially (faster than Cu and Ni dissolve into the Sn) into the surface of the solid Cu-Ni reinforcement powder above the matrix alloy liquidus temperature [1,17,18,19] to form a Cu-Ni-Sn solid solution. However, what was observed was that both Cu and Ni diffused preferentially into the Sn so that the resulting alloy phase, essentially the entire matrix, was $Cu_{5.5}Ni_{0.5}Sn_5$, a fully substituted ternary intermetallic compound. This transformation raised the minimum melting temperature of the system post-reflow from 227°C for the original SN100C solder matrix alloy [3,21] to approximately 415°C (based on the melting temperature of Cu_6Sn_5) [3] for the $Cu_{5.5}Ni_{0.5}Sn_5$ phase. This gives the resulting solder joint the ability to withstand higher operating temperatures and Joule heating [18]. Moreover, the data shows (see Fig. 9), that longer times and/or higher reflow temperatures both increase the vol.% of ternary IMC and decrease the Cu-10Ni loading, both of which can degrade the desired joint properties. Therefore, from the available data, the lowest reflow temperature, 250˚C, and the shortest time, 30 seconds are recommended as most suitable for initial joint fabrication.

For this study, the term liquid-phase diffusion bonding or LPDB was coined to more accurately represent the phenomenon occurring within this composite microstructure between the melted solder alloy matrix and the slowly dissolving Cu-10Ni powders. Thus, a major portion of the bonding process actually involves rapid volume diffusion through the resulting intermetallic compound (IMC) phase that forms immediately upon melting of the solder alloy, rather than by the surface diffusion mechanism usually associated with solid-state sintering. It is quite interesting (see Fig. 9) that after only 30s at a peak reflow temperature of 250˚C, the molten Sn-alloy matrix is converted almost completely into the ternary IMC, with only 4% of the original 30% of solder alloy remaining untransformed. This was accompanied by a

loss of about 4% of the volume fraction of the Cu-10Ni alloy powder, which provided the excess Cu and Ni needed to accomplish this rapid growth of the IMC by what we assume is a volume diffusion process through the ternary IMC layer. Therefore, this example of the LPDB process (see Fig.11) refers to enhanced diffusion of Cu and Ni atoms from the solid Cu-10Ni reinforcement powder through a growing IMC layer to (eventually) consume the low-melting alloy matrix at a rather low temperature. For this system, it appears that a typical reflow temperature (250˚C) for SN100C solder is sufficient to encourage adequate solid-state diffusion to form a continuous conductive network throughout the composite solder joints. With LPDB, we still focus on the liquid-phase change of the matrix, but give interdiffusion the credit it deserves.

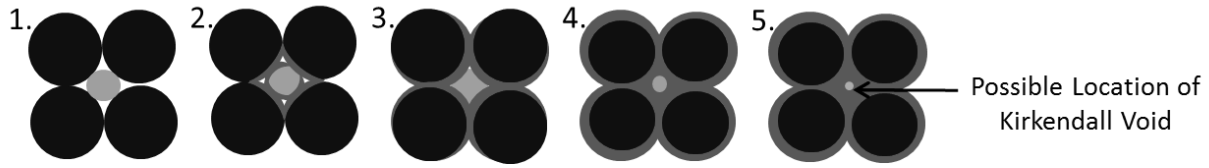

Figure 11: *The process of liquid-phase diffusion bonding of Cu-10Ni powders and SN100C powders: 1. Two types of powder are blended (light gray=low-melting tin alloy, black=high-melting Cu-10Ni); 2. Diffusion between Sn alloy and Cu-10Ni particles at points of contact during initial heating; 3. Capillary liquid spreading of tin alloy upon melting; 4. Completion of isothermal solidification of IMC (intermediate gray) upon cooling; 5. Possible location of Kirkendall void with TLPS [19,21].*

Indicated in Fig. 11 is a possible location that Kirkendall or diffusion-related voids could form in our system with TLPS. Upon melting of the tin alloy around 227°C and heating to reflow at 250˚C, the tin atoms could begin to diffuse into the solid Cu-Ni particles [3,19,21]. In contrast, we observed that the copper and nickel atoms appear to be dissolving preferentially into the Sn-rich matrix (forming $Cu_{5.5}Ni_{0.5}Sn_5$) with a faster flux rate than the Sn atoms are diffusing into the solid Cu-Ni. In fact, semi-quantitative chemical analysis in the SEM of the retreating Cu-Ni phase in the microstructures show only a trace of 0.1 at.% Sn (which is probably from EDS detection error) in the Cu-Ni phase, post-reflow. This dominance of the diffusive flux of Cu and Ni over the Sn flux is likely due in part to the relatively large atomic (metallic) radius of tin (1.542 Å) compared to copper (1.276 Å) and nickel (1.244 Å) [22] and the high driving force to form the ternary intermetallic. With this observed interdiffusion phenomenon of LPDB, no observation was made of Kirkendall voiding usually seen at interfaces between phases, a apparent benefit of this innovative solder system [19,21].

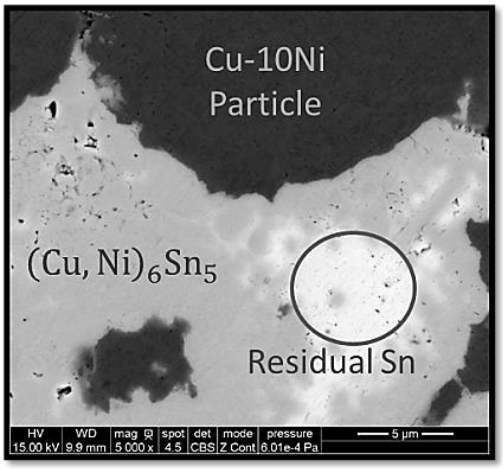

Figure 12: *This image shows how the reinforcement powders (the darkest regions of the microstructure) diffuse into the liquid tin alloy, creating $(Cu,Ni)_6Sn_5$. The circle is one location susceptible with TLPS to*

Kirkendall voiding when the residual tin is completely diffused into the intermetallic. Clearly, no voiding occurs due to the Cu and Ni invasion of this area to form the IMC.

We also clearly see microstructural evidence (see Fig. 8 and 12) that there is no cracking of the ternary IMC in the joint cross-section, which is consistent with the previously observed effect of Ni substitution on suppression of the hexagonal transformation to monoclinic in Cu_6Sn_5 that causes cracking (see Fig. 3), as mentioned in the introduction. Thus, there can certainly be a benefit on mechanical properties (e.g., fatigue and shock resistance) that would be expected in solder joints made from this new composite paste system.

Advantages of this Pb-free, environmentally-friendly solder paste model system, in addition to a lower reflow temperature, a shorter reflow time, and a much higher melting temperature for the resulting intermetallic phase with increased ductility, are that the thermal expansion of the solder and most ceramic substrates are more equally matched and the strength of the solder joint theoretically increases. Estimates of the thermal expansion mismatch show a mismatch of 20-25 ppm/°C between Pb-5Sn and alumina and a mismatch of only 5-10 ppm/°C between Cu-10Ni and alumina [9,23,24]. Estimates of shear modulus for Pb-5Sn and Cu-10Ni show values on the order of 5 GPa and 50 GPa [24], respectively [21]. These values of CTE and shear modulus from literature vary between experimental and calculated data. Some of these estimated values are only based on a "rule of mixtures" approach and remain to be experimentally tested on the full composite joint microstructure; however, the ranges in data indicate a large enough difference in values that an improvement in properties can still be hypothesized due to the lowering of the interfacial stress for a given temperature change.

CONCLUSION

In conclusion, it has been verified that the dual-phase low melting solder paste model (SN100C/Cu-10Ni) transforms to an acceptable composite solder joint microstructure for high temperature use. To verify this prediction, we have proposed to make a lead-free solder paste that contains 70 volume percent Cu-10Ni powder blended with 30 volume percent SN100C powder. The resulting IMC composition of this solder paste system has an approximate 5 at.% content of Ni and showed no cracking due to the added nickel that suppresses the IMC phase transformation [6]. Our paste technology uses a peak reflow temperature of 250°C, but can be used up to 415°C [3]. Due to this, we can say we have the potential for a practical and suitable lead-free alternative high temperature solder with improved processing parameters.

ACKNOWLEDGEMENTS

The authors would like to thank the Iowa State University Research Foundation (ISURF) and Nihon-Superior, Inc. Ltd., through the Ames Lab contract (DE-AC02-07CH11358) for their support.

REFERENCES

1. Chidambaram, Vivek, Jesper Hattel, and John Hald. "High-Temperature Lead-Free Solder Alternatives." *Microelectronic Engineering*. 88 (2011) 981-989.
2. Gayle, Frank W., Gary Becka, Jerry Badgett, Gordon Whitten, Tsung-Yu Pan, Angela Grusd, Brian Bauer, Rick Lathrop, Jim Slattery, Iver Anderson, Jim Foley, Alan Gickler, Duane Napp, John

Mather, and Chris Olson. “High-Temperature Lead-Free Solder for Microelectronics.” *JOM*. June 2001, pp.17-21.
3. McCluskey, Patrick and Hannes Greve. “Transient Liquid Phase Sintered Joints for Wide Bandgap Power Electronics Packaging.” *Pan Pacific Symposium Conference Proceedings*. 11 February 2014.
4. Palmer, A. Mark, Nicole S. Erdman, and David A. McCall. “Forming high Temperature Solder Joints through Liquid Phase Sintering of Solder Paste.” *Journal of Electronic Materials*. Vol. 28, No.11, 1999.
5. Tsai, Tsung-Nan. “Thermal Parameters Optimization of a Reflow Soldering Profile in Printed Circuit Board Assembly: A Comparative Study.” *Applied Soft Computing.* 12 (2012) 2601-2613.
6. Nogita, Kazuhiro. “Stabilisation of Cu_6Sn_5 by Ni in Sn-0.7Cu-0.05Ni Lead-Free Solder Alloys.” *Intermetallics*. 18 (2010) 145-149.
7. Nogita, Kazuhiro, Stuart D. McDonald, Hideaki Tsukamoto, Jonathan Read, Shoichi Suenaga, and Tetsuro Nishimura. “Inhibiting Cracking of Interfacial Cu_6Sn_5 by Nickel Additions to Sn-based Lead-Free Solders.” *The Japan Institute of Electronics Packaging.* Vol. 2, No.1, 2009.
8. Sweatman, Keith. “Another Chance for Tin-Copper as a Lead-free Solder.” *APEX Special Issue*. February 2005.
9. Sweatman, Keith, Tetsuro Nishimura, Stuart D. McDonald, and Kazuhiro Nogita. “Effect of Cooling Rate on the Intermetallic Layer in Solder Joints.” *IPC APEX EXPO Proceedings.*
10. I.E. Anderson, “Development of Sn-Ag-Cu and Sn-Ag-Cu-X alloys for Pb-free electronic solder applications,” J. Mater. Sci: Mater. Electron. (2007) 18, pp. 55-76.
11. I.E. Anderson, J.W. Walleser, J.L. Harringa, F. Laabs, A. Kracher, “Nucleation Control and Thermal Aging Resistance of Near-Eutectic Sn-Ag-Cu-X Solder Joints by Alloy Design,” JEM, (2009) 38 (12), pp. 2770-2790.
12. Nogita, Kazuhiro and Tetsuro Nishimura. “Nickel-Stabilised Hexagonal $(Cu,Ni)_6Sn_5$ in Sn-Cu-Ni Lead-Free Solder Alloys.” *Scripta Materialia*. 59 (2008) 191-194.
13. Sheng Liu, Chao, Cheng En Ho, Cheng Sam Peng, and C. Robert Kao. “Effects of Joining Sequence on the Interfacial Reactions and substrate Dissolution Behaviors in Ni/Solder/Cu Joints.” *Journal of Electronic Materials*. Vol.40, No.9, 2001.
14. Labie, Riet, Wouter Ruythooren, and Jan Van Humbeeck. “Solid State Diffusion in Cu-Sn and Ni-Sn Diffusion Couples with Flip-Chip Scale Dimensions.” *Intermetallics.* 15 (2007) 396-403.
15. Park, M.S. and R. Arróyave. “Early Stages of Intermetallic Compound Formation and Growth during Lead-Free Soldering.” *Acta Materialia* 58 (2010) 4900-4910.
16. Ventura, Tina, Sofiane Terzi, Michel Rappaz, and Arne K. Dahle. “Effects of Ni Additions, Trace Elements, and Solidification Kinetics on Microstructure Formation in Sn-0.7Cu Solder.” *Acta Materialia* 59 (2011) 4197-4206.
17. Bader, S., W. Gust, and H. Hieber. “Rapid Formation of Intermetallic Compounds by Interdiffusion in the Cu-Sn and Ni-Sn Systems.” *Acta Metall. Mater.* Vol. 43, No.1, pp. 329-337, 1995.
18. Corbin, S.F. “High-Temperature Variable Melting Point Sn-Sb Lead-Free Solder Pastes Using Transient Liquid-Phase Powder Processing.” *Journal of Electronic Materials.* Vol. 34, No.7, 2005.
19. Corbin, S.F. and P. Lucier. “Thermal analysis of Isothermal Solidification Kinetics during Transient Liquid-Phase Sintering.” *Metallurgical and Materials Transactions A.* Volume 32A, April 2001. Pp 971.
20. Lumley, R.N. and G.B. Schaffer. “The Effect of Solubility and Particle Size on Liquid-Phase Sintering.” *Scripta Materialia.* Vol. 35, No. 5, pp. 589-595. 1996.
21. Qiao, X. and S.F. Corbin. “Development of Transient Liquid Phase Sintered (TLPS) Sn-Bi Solder Pastes.” *Materials Science and Engineering* A283 (2000) 38-45.
22. Pauling, Linus. “Atomic Radii and Interatomic Distances in Metals.” *J. Am. Chem. Soc.* March 1947, 69(3), pp 542-553.
23. Mu, Dekui, Jonathan Read, Yafeng Yang, and Kazuhiro Nogita. “Thermal Expansion of Cu_6Sn_5 and $(Cu,Ni)_6Sn_5$.” *Journal of Materials Research*. Vol. 26, No. 20, Oct 28, 2011.

24. Siewert, Thomas, Stephen Liu, David R. Smith, and Juan Carlos Madeni. “Properties of Lead-Free Solders Release 4.0.” *Database for Solder Properties with Emphasis on New Lead-Free Solders through the National Institute of Standards and Technology and Colorado School of Mines.* Colorado. 11 February 2002.